Performance Analysis of a Horizontal Anode Baking Furnace for Aluminum Production

Abdul Raouf Tajik[1], Tariq Shamim[2], Rashid K. Abu Al-Rub[3] and Mouna Zaidani[4]
1. Ph.D. Student
2. Professor
3. Department Head and Associate Professor
4. Postdoctoral Researcher
Institute Center for Energy (iEnergy), Department of Mechanical and Materials Engineering,
Masdar Institute of Science and Technology, Abu Dhabi, U.A.E.
Corresponding author: tshamim@masdar.ac.ae

Abstract

Anode baking is the most expensive and the most important step during carbon anode production. The operational-geometrical parameters have significant influence on the anode baking furnace performance and carbon anode quality. Numerical modelling is an imperative tool to investigate the effect of different parameters on anode baking process. In the present study, a numerical model is developed which simulates heat transfer and flow distributions of the entire anode baking process. Using this numerical model, effect of various factors on anode temperature distribution is studied. Impact of degraded refractory-wall thermal conductivity on baking process is investigated and it is observed that for the aged furnaces this material properties degradation should be addressed accordingly. During the preheating and firing sections the temperature drops drastically from flue-gas to the center of the anode through the width of the pit which indicates a huge loss of energy. Calculating temperature standard deviation for the entire baking process, it is observed that the temperature non-uniformity presents mostly in the refractory wall and packing coke regions, and anode experiences a homogenous temperature distribution.

Keywords: Flue-wall; air infiltration; anode baking; volatiles combustion; packing coke.

1. Introduction

In aluminium industry, for each ton of aluminium to be produced approximately 0.4 ton of carbon anodes are consumed in the reduction cell. Green (unbaked) anodes should be baked (heat treated) in advance to obtain particular mechanical, thermal and electrical properties that make them suitable to be used as anode in the aluminium production process. The anode baking process takes generally 390-480 hours, and several phenomena occur during the process. Effects of operational-geometrical parameters on the performance of the furnace by plant tests are usually expensive and disrupt the baking process. Therefore, numerical-mathematical modelling is an imperative tool to study the effect of different parameters on the anode quality and furnace performance. Ultimately the optimum baking process and furnace geometry can be proposed. Several studies on modelling the anode baking process are reported in the literature [1-8]. The main objectives of the developed computational model are to study the effect of material properties on the baking process, to investigate the effect of various parameters on anode temperature distribution, and to investigate the temperature evolution through the width of the pit.

2. Model Description

Anode baking furnace is a circular kiln with pits, analogous to a closed chain. As shown in Figure 1, a fire group usually consists of three preheating sections, three firing sections, six

cooling sections, one unloading section, one or two sections for the loading of green anodes and one or two sections for the sake for maintenance. After each fire cycle time (typically 24-32 hours), the fire group equipment is displaced one section forward in the direction of the fire advance which is typically clockwise direction. A furnace comprises of two fire groups where the sections are arranged in two rows side by side, joined at the two ends by the crossover. The fire advance direction and the flow direction of combustion air and flue gases in the flue walls is the same. Simulating this intermittent movement of the fire group along with all the other simultaneous and transient phenomena involved in the baking process is very challenging and at the same time computationally very intensive since the initial and boundary conditions are continuously varying from one section to another. In a view to overcome this difficulty, all the sections from preheating, firing to cooling are treated as a whole and the baking furnace is assumed to be a semi-continuous counter flow heat exchanger between the stepwise movement of the solids in the pit and continuous flow of the gas in the flue. However, to avoid the virtual movement of the anodes, the solids are fictitiously subdivided into a number of finite slices along the length of the furnace. The velocity of the gas is varying and is determined by considering the local mass flow rate, temperature and pressure. The constant velocity of the solids is equal to a section length divided by the fire cycle time (about 5 m per day).

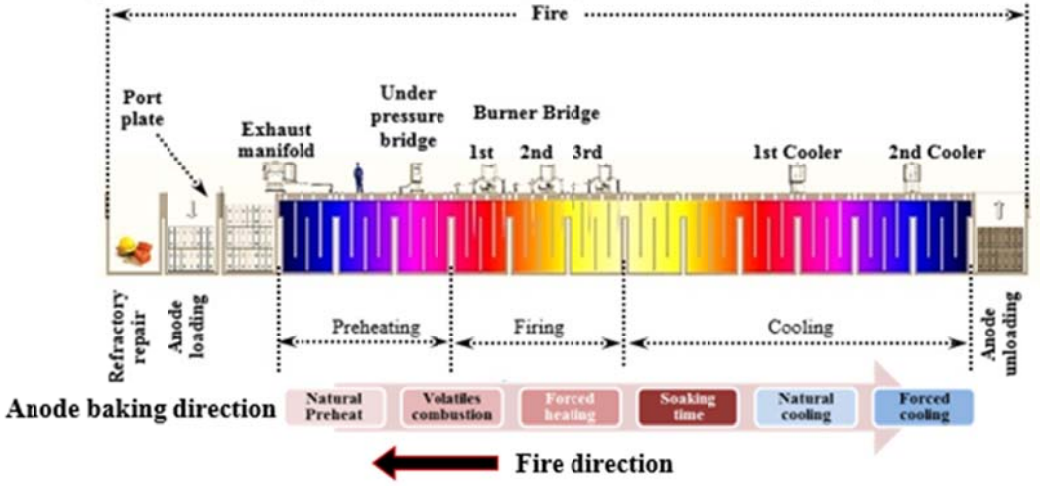

Figure 1. Longitudinal view of all the sections in a fire group [9]

2.1. Coupling of the flue and pit models

The transient nature of the anode baking process should be taken into consideration while developing the computational algorithms for the model. Assuming symmetry, only half of the flue and half of the pit can be considered for the computation. The time scale of the gas is much smaller than that of the solid materials (i.e. the solid components take more time to respond to changes in boundary conditions whereas gas responds to variations quickly). Combustion of fuel and volatiles in the flue along with gas flow combined with air in-leakage and ex-leakage can be modelled independent of time. However, the transient (time-dependent) heat conduction equation should be solved for the pit sub-model (i.e., heat transfer through the flue-wall, packing coke, and anode pack). Thus, the developed numerical model consists of two sub-models: flue and pit (flue-wall, packing coke, and anode pack). As shown in Figure 2, the pit model and flue model are developed separately and then coupled through an interface located at the refractory wall surface on the flue side.

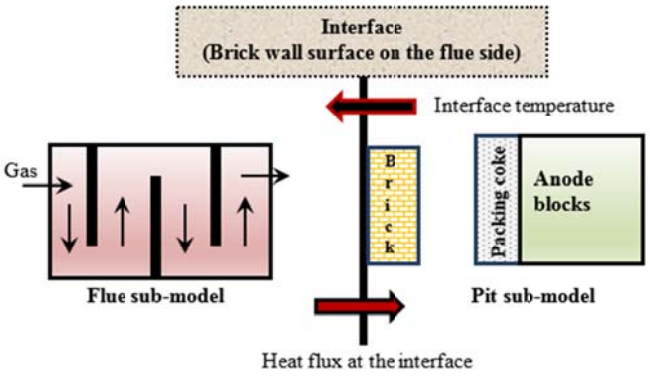

Figure 2. Coupling of the flue and pit sub-models.

As illustrated in Figure 3, in the preheating and firing zones the heat is transferred form flue gases to the refractory walls by convection and radiation, and then by conduction to the packing coke and anodes, and vice-versa for the cooling sections.

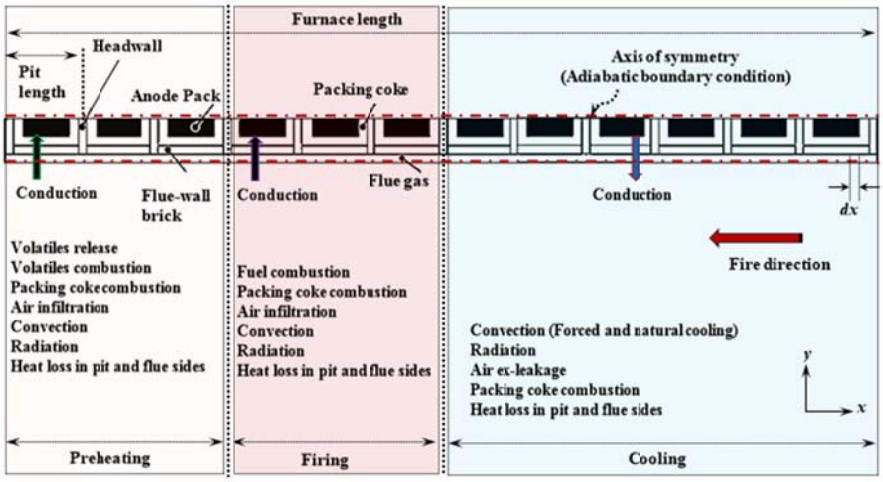

Figure 3. Schematic representation of the model's domain.

2.2. Governing equations

The followings are the governing equations that are solved for the modelling of the anode baking process. Figure 4-a, shows schematic view of 1D domain for heat conduction in the traversal direction, perpendicular to fire direction. 1D transient heat conduction equation can be written as:

$$\rho_s C_{ps} \frac{\partial T_s}{\partial t} = \frac{\partial}{\partial y}\left(k_s \frac{\partial T_s}{\partial y} \right) - Q_{P-lost} \qquad (1)$$

Where,

k_s : Thermal conductivity of the solids (wall, packing coke and anodes), (W/m. $^{\circ}$C)

C_{ps} : Specific heat of the solids (J/kg. $^{\circ}$C)

ρ_s : Density of the solids (kg/m^3)

T_s : Solids temperature (°C)

Q_{P-lost} : Heat loss to the atmosphere from bottom and top of the pit (W/m^3)

t : Time (s)

y : Transversal co-ordinate perpendicular to the fire direction (m)

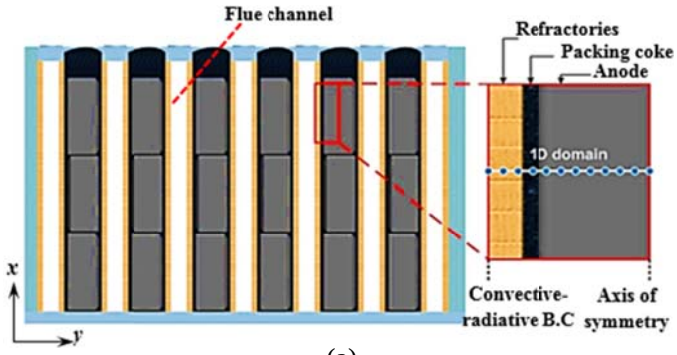

(a)

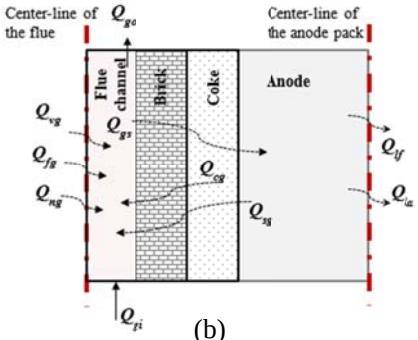

(b)

Figure 4. (a) Schematic view of 1D heat conduction domain (b) Schematic of the gas control volume.

The adiabatic boundary condition is adopted for the axis of the symmetry at the centre of the anode. The interface between flue-gas and refractory wall is treated as convective-radiative boundary condition (see Figure 4-a). As shown in Figure 4-b, for a slice of the flue-wall of thickness "dx", the heat balance equation can be written as the total heat coming into the gas control volume is equal to the heat leaving the control volume, which can be described using the following equation [1-8]:

$$\overbrace{\left(Q_{gi}-Q_{go}\right)}^{flue\ gas}-\overbrace{Q_{ng}}^{\text{infiltrated air}}-\overbrace{\left(Q_{sg}-Q_{gs}\right)}^{Heat\ transfer\ from\ flue\ gas\ to\ wall}+\overbrace{Q_{fg}}^{Heat\ provided\ by\ the\ fuel}+\overbrace{Q_{vg}}^{Heat\ provided\ by\ the\ volatiles\ combusted}$$
$$+\overbrace{Q_{cg}}^{Heat\ provided\ by\ the\ packing\ coke\ combusted}-\overbrace{\left(Q_{lf}+Q_{la}\right)}^{Heat\ loss\ to\ atmosphere\ and\ foundation}=0 \qquad (2)$$

Substituting physical expression of the terms mentioned in the Eq. (2), it can be expressed as:

1. For the preheating sections

$$\overbrace{\dot{m}_g C_{pg} \frac{dT_g}{dx}}^{\text{flue gas}} + \overbrace{\eta_1 \dot{m}_c H_c}^{\text{Heat provided by the coke}} + \overbrace{\eta_2 \left(\dot{m}_{tar} H_{tar} + \dot{m}_{CH_4} H_{CH_4} + \dot{m}_{H_2} H_{H_2} \right)}^{\text{Heat provided by the volatiles combusted}} - \overbrace{\dot{m}_n C_{pg} (T_g - T_\infty)}^{\text{infiltrated air}} - \overbrace{2 h_T D_{\text{flue}} (T_g - T_w)}^{\text{Heat transfer from flue gas to wall}} - \overbrace{Wh_{equiv} (T_g - T_\infty)}^{\text{Heat loss to atmosphere and foundation}} = 0 \quad (3)$$

2. For the firing sections

$$\overbrace{\dot{m}_g C_{pg} \frac{dT_g}{dx}}^{\text{flue gas}} + \overbrace{\eta_1 \dot{m}_c H_c}^{\text{Heat provided by the coke}} + \overbrace{\eta_3 \dot{m}_f H_f}^{\text{Heat provided by the fuel}} - \overbrace{\dot{m}_n C_{pg} (T_g - T_\infty)}^{\text{infiltrated air}} - \overbrace{2 h_T D_{\text{flue}} (T_g - T_w)}^{\text{Heat transfer from flue gas to wall}} - \overbrace{Wh_{equiv} (T_g - T_\infty)}^{\text{Heat loss to atmosphere and foundation}} = 0 \quad (4)$$

3. For the cooling sections

$$\overbrace{\dot{m}_g C_{pg} \frac{dT_g}{dx}}^{\text{flue gas}} + \overbrace{\eta_1 \dot{m}_c H_c}^{\text{Heat provided by the coke}} - \overbrace{2 h_T D_{\text{flue}} (T_g - T_w)}^{\text{Heat transfer from flue gas to wall}} - \overbrace{Wh_{equiv} (T_g - T_\infty)}^{\text{Heat loss to atmosphere and foundation}} = 0 \quad (5)$$

Where,

η_1 : Percentage of packing coke that combusts, (.)

η_2 : Percentage of volatile release that combusts in the flue, (.)

η_3 : Combustion efficiency, (.)

W : Flue width, (m)

P_{flue} : Equivalent perimeter of the flue, (m)

T_g : Gas temperature, (°C)

h_T : Total heat transfer coefficient (Convective and Radiative), (W/m^2. °C)

$\dot{m}_g$: Gas mass flow in the flue, (kg/m. s)

$\dot{m}_f$: Fuel injection per unit furnace length, (kg/m. s)

$\dot{m}_v$: Volatiles release rate per unit furnace length, (kg/m. s)

c_{pg} : Specific heat of the gas, (J/kg. °C)

T_w : Wall temperature, (°C)

H_f and H_v : Fuel and volatiles gases heats of reaction (J/kg)

h_{equiv} : Equivalent heat transfer coefficient; considering the conductive resistance of the top and bottom solid materials, and convective- radiative heat transfer from top and bottom, (W/m^2. °C)

The total heat transfer coefficient h_T is given as the sum of convective and radiative heat transfer coefficients. During the baking process, the mass flow rate of the flue-gas inside the flue wall is a function of the draft level, the design of the flue channel and sealing of the furnace at the sources of the air infiltration such as head wall openings (placing coolers or exhaust manifolds), peep-hole openings (placing burners), porous media (packing coke) and cracks through the brick and concrete flue tops.

The green anodes are heat treated in anode baking furnace during the pre-heating and firing zones with the heat provided by the pitch volatiles and fuel combustion respectively. The volatile matters in green anodes are composed of methane, hydrogen and tar. The purpose of the baking process is to convert the coal tar pitch binder into high quality binder coke which holds the filler coke particles together. The amount of volatiles released is a function of the anode temperature and mass of the stored volatiles in the green anode. The volatile release rate can be expressed as follows [8]:

$$\dot{m}_v = \frac{\partial m_v}{\partial T_a}\frac{\partial T_a}{\partial t} = \frac{\partial m_v}{\partial t} \qquad (6)$$

Where,

T_a : Anode temperature (°C)

3. Results and Discussion

Figure 5 shows the comparison between the calculated anode average temperature with that of reported by Severo and Gusberti [8]. It can be observed that there is a good agreement between the two results.

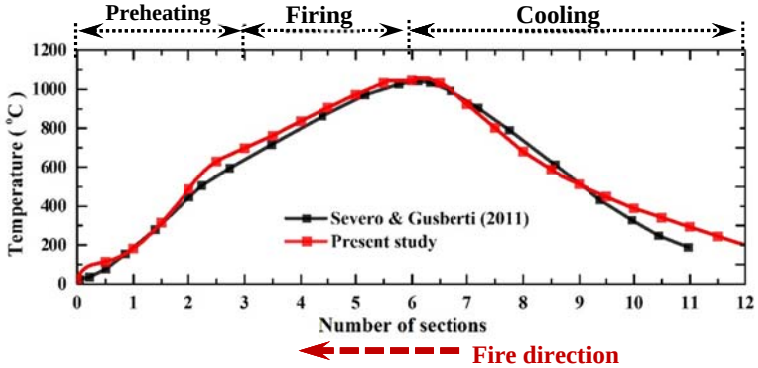

Figure 5. Comparison of calculated and reported anode average temperature.

During the anode baking process, the main concern is to maintain the prescribed temperature curves. The heat-up rate of the anode should not exceed the critical range. It takes typically 24–48 hours for anodes to reach the flue-gas temperature. Hence,

considering the anode temperature as the input signal for the control system of the baking process is not feasible. Therefore, the pre-defined anode temperature curve has to be translated into the flue gas temperature curve. Figure 6 shows the calculated flue-gas, refractory wall, packing coke, and anode average temperature distribution obtained.

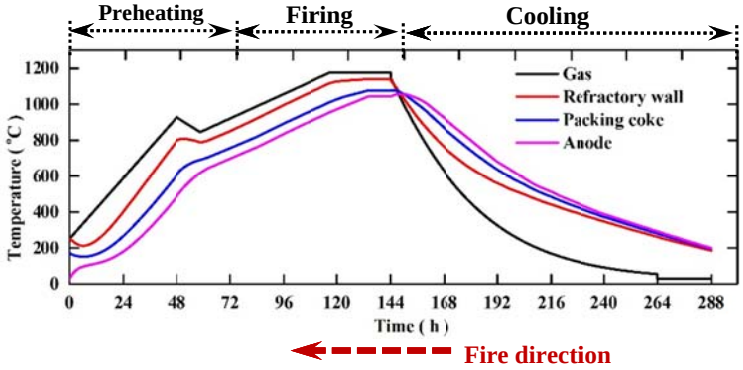

Figure 6. Gas, flue-wall and anode average temperature.

Using line plots, average temperature can only be depicted. Figure 7 illustrates the temperature contour for refractory-wall, packing coke and anode packing during the entire baking process.

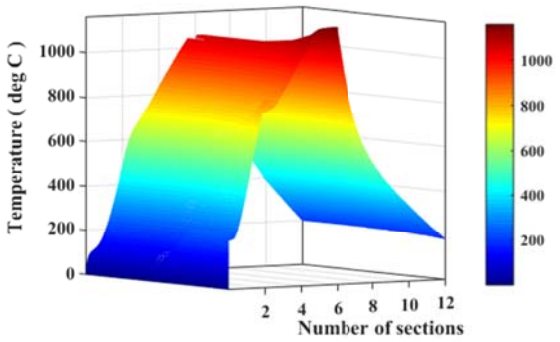

Figure 7. Three dimensional view of the solids temperature distribution.

Using this type of data representation, the local solids temperature distribution in the whole computational domain can be presented, and hot spots and low temperature zones can be identified.

3.1. Constant and variable material properties

The anode average temperature for constant and time dependent material properties are considered. The data for material properties is taken form Severo & Gusberti [8]. As shown in Figure 8 for constant material properties three different cases are considered: Taking the properties:

1. At 20 °C,
2. At 1000 °C,
3. Average values from 20 °C to 1000 °C.

It can be observed from Figure 8 that while considering constant material properties the results obtained for case 2 and 3 show better agreement with that of temperature dependent case.

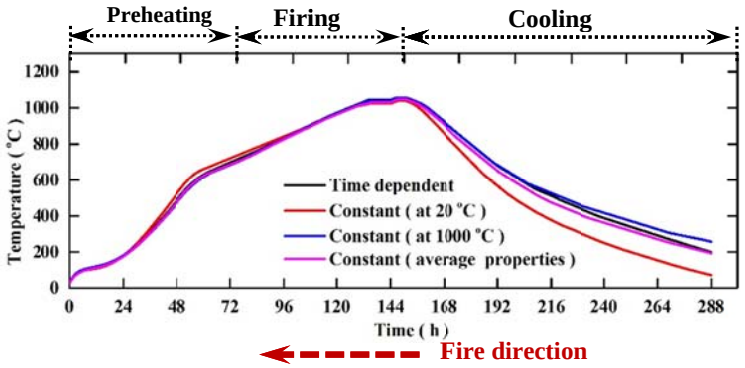

Figure 8. Anode average temperature while considering constant and time dependent material properties.

3.2. Effect of aging on solids temperature distribution

The complex corrosion behaviour of fireclay bricks is determined by various individual interacting processes. The properties of the refractory bricks influence sensibly the wear of the flues, high flue gas temperature and other factors. In a view to address this issue, it is considered that a portion of the refractory wall material properties is degraded. As shown in Figure 9, this degradation has significant effect on anode temperature distribution and should be incorporated into the model while using the model for the aged furnaces.

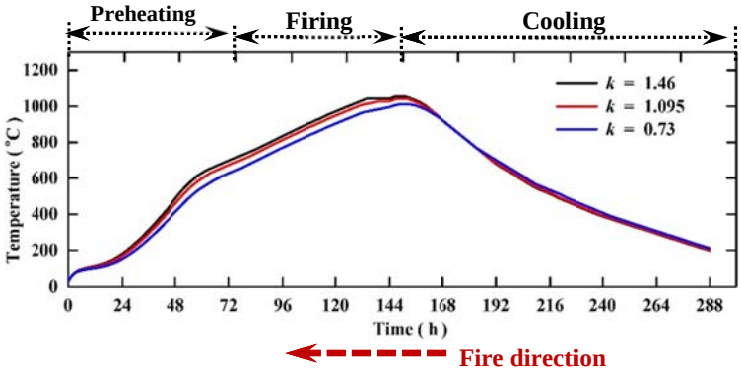

Figure 9. Effect of refractory-wall thermal conductivity degradation on anode average temperature.

3.3. Effect of varying operational and geometrical parameters on anode temperature

Figure 10 shows effect of varying soaking time, anode size, section length and packing coke thickness on anode average temperature. As shown the anode temperature distribution is significantly affected by varying the above mentioned parameters.

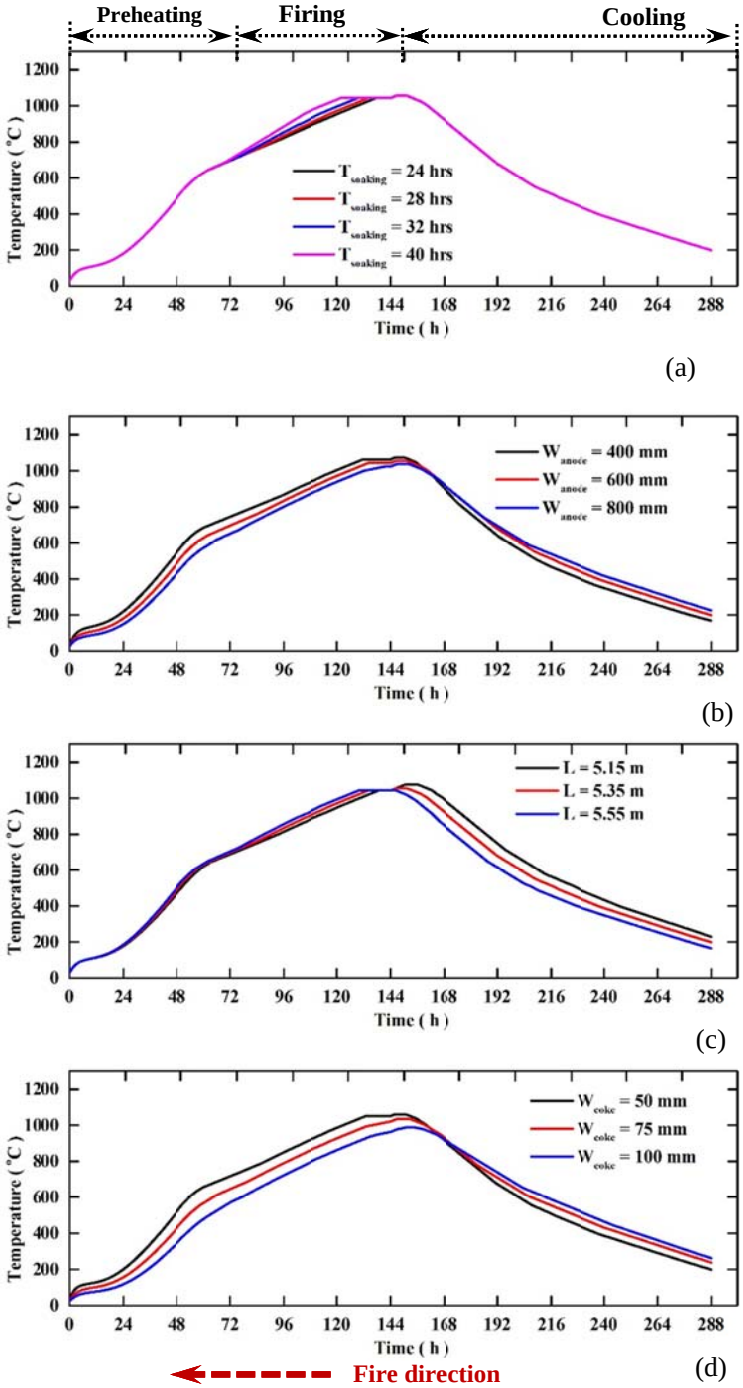

Figure 10. Effect of varying a) soaking time b) anode pack size c) section length d) packing coke thickness, on anode average temperature.

3.4. Temperature evolution through the width of the pit

Figure 11 shows the drop in temperature from flue-gas to middle of the anode ($T_{flue-gas} - T_{anode}$) through the width of the pit during the baking process. It can be observed that during preheating

and firing sections a large drop in temperature is occurring. This temperature drop indicates a huge energy loss which should be minimized during the baking process.

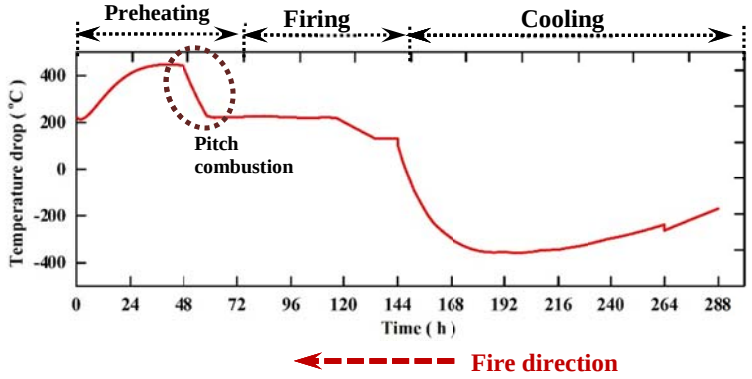

Figure 11. Temperature drop from flue-gas to the centre of the anode ($T_{flue-gas} - T_{anode}$) through the width of the pit.

As illustrated in Figure 12 during the preheating and firing sections, flue-gas to solid temperature drop is maximum during the initial anode heat-up and pitch volatiles combustion, and reduces during the last firing section (soaking time).

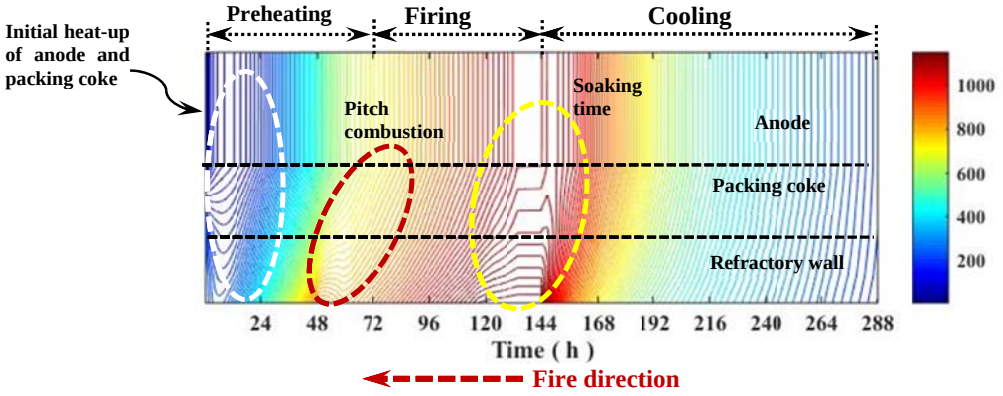

Figure 12. Solids temperature evolution through the width of the pit.

Calculating standard deviation (*SD*) of the temperature within the solid parts can be a good indication of the temperature non-homogeneity while operating parametric studies on anode baking process.

$$SD = \sqrt{\frac{1}{N}\sum_{i=1}^{N}(T_i - T_{avr})} \qquad (7)$$

Where,
SD: Standard deviation
N: Number of nodes
T_i : Temperature values at each node for the solids (refractory wall, packing coke, anode)
T_{avg} : Average temperature

As shown in Figure 13-a, the *SD* values for refractory wall and packing coke regions are as high as 70 °C, which indicates a high temperature non-uniformity. On the other hand, anode experiences almost a homogenous temperature distribution (see Figure 13-b).

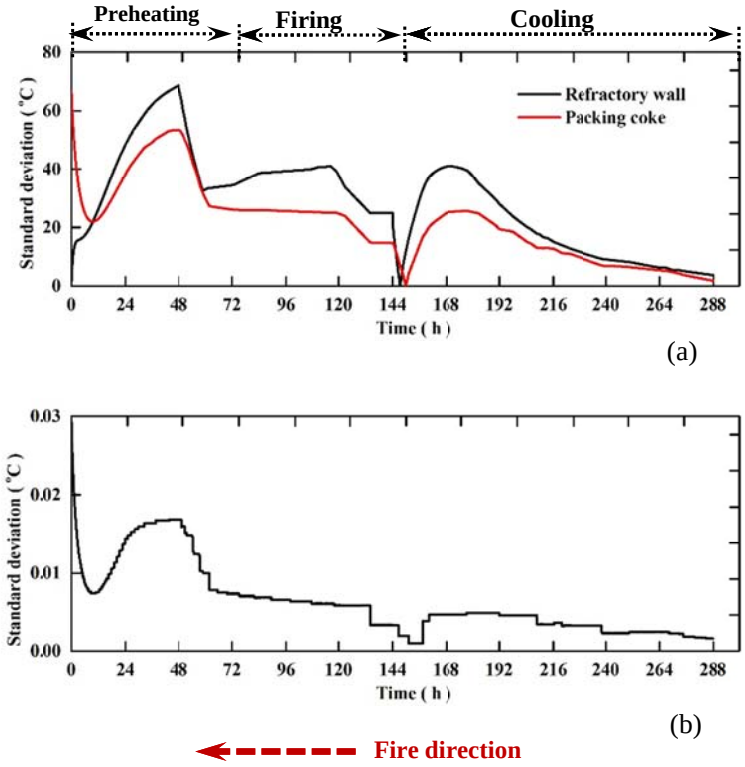

Figure 13. *SD* distribution for a) Refractory wall & packing coke, b) Anode.

4. Conclusions

In the present study a numerical model is developed for the anode baking process. Effect of various operational/geometrical parameters on anode average temperature are investigated. It is observed that degradation of refractory wall properties has significant effect on anode temperature distribution and should be addressed accordingly. The standard deviation of the solid temperature is calculated and it is observed that during the preheating and firing sections, the *SD* values is maximum during the initial heat-up and pitch volatiles combustion and reduces at the end of the firing sections.

The developed numerical model can be used to as an effective tool to enhance the overall furnace efficiency, to improve the anode quality and to maximize the carbon anode production.

5. Acknowledgements

The authors acknowledge the support from the Emirates Global Aluminium (EGA).

6. References

1. R. Bui, A. Charette, T. Bourgeois, Simulating the process of carbon anode baking used in the aluminum industry, *Metallurgical Transactions B*, 15 (1984) 487-492.
2. R. Bui, A. Charette, T. Bourgeois, E. Dernedde, Performance analysis of the ring furnace used for baking industrial carbon electrodes, *The Canadian Journal of Chemical Engineering*, 65 (1987) 96-101.
3. R. Bui, E. Dernedde, A. Charette, T. Bourgeois, Mathematical simulation of a horizontal flue ring furnace, *Essential Readings in Light Metals: Electrode Technology for Aluminum Production*, Volume 4, (1984) 386-389.
4. R.T. Bui, A. Chartette, T. Bourgeois, A computer model for the horizontal flue ring furnace, *Industry Applications, IEEE Transactions on*, (1984) 894-901.
5. A. Charette, R.T. Bui, T. Bourgeois, Modeling the heat transfer in a ring furnace, *Industry Applications, IEEE Transactions on*, (1984) 902-907.
6. N. Oumarou, Y. Kocaefe, D. Kocaefe, B. Morais, J. Lafrance, A Dynamic Process Model for Predicting the Performance of Horizontal Anode Baking Furnaces, *Light Metals* 2015, 1079-1086.
7. L. Zhang, C. Zheng, M. Xu, Simulating the heat transfer process of horizontal anode baking furnace, *Developments in Chemical Engineering and Mineral Processing*, 13 (2005) 447-458.
8. D.S. Severo, & Gusberti, V., User-friendly software for simulation of anode baking furnaces, in: Proceeding of 10th Australian conference, 2011.
9. Akhtar, R. J., Meier, M. W., Sulger, P. O., Fischer, W. K., Friedrich, R., & Janousch, T. (2012). Anode Quality and Bake Furnace Performance of EMAL. *Light Metals*, 1175-1179.